ISSN 0001-4338, Izvestiya, Atmospheric and Oceanic Physics, 2025, Vol. 61, No. 4, pp. 431–445. © Pleiades Publishing, Ltd., 2025.

Efficiency of Photochemical Production of Ozone in the Near-Surface Air Layer in Boreal Forests of Central and Southern Siberia

K. B. Moiseenko[a], *, A. V. Vasileva[a], I. B. Belikov[a], E. V. Berezina[a], M. Yu. Arshinov[b], and B. D. Belan[b]

[a] *Obukhov Institute of Atmospheric Physics, Russian Academy of Sciences, Moscow, 119017 Russia*

[b] *Zuev Institute of Atmospheric Optics, Siberian Branch, Russian Academy of Sciences, Tomsk, 634055 Russia*

**e-mail: k_moeseyenko@ifaran.ru*

Received October 24, 2024; revised December 20, 2024; accepted December 27, 2024

Abstract—Estimates of photochemical ozone production rate (P_{O_3}), ozone production efficiency (OPE) per one molecule of odd nitrogen NO_x (=NO + NO_2) (ΔP), and NO_x exponential lifetime (τ_N) in photochemically active days from March to September are obtained from long-term observations of near-surface content of ozone (O_3) and nitrogen oxides (NO and NO_2) at the regional stations ZOTTO (ZOtino Tall Tower Observatory, Central Siberia) and Fonovaya (Southern Siberia). In the range of the measured NO_x mixing ratios (0.2–2 ppb) corresponding to conditions of regionally background and weakly contaminated air, the dependences $P_{O_3} \approx A' \cdot [NO_x]$, $\Delta P = A/(1 + B[NO_x])$, and $\tau_N = \Delta P/A'$ are valid, where A' is an empirical coefficient and A and B are parameters dependent on the air composition. For the odd nitrogen family, limit regimes of the photochemical sink rate under conditions of high and low ratios of the concentration of biogenic hydrocarbons to the NO_x concentration are revealed. The obtained results show the significant contribution of regional NO_x emissions and biogenic emissions of hydrocarbons to photochemical production of ozone and daytime sink of odd nitrogen in the atmospheric boundary layer over boreal forests of Siberia.

Keywords: ozone, nitrogen oxides, tropospheric photochemistry, regional emissions, volatile organic compounds, ozone precursors, atmospheric boundary layer

DOI: 10.1134/S000143382570077X

INTRODUCTION

The content of tropospheric ozone (O_3) and nitrogen oxides (NO_x = NO + NO_2) is among most important factors determining the oxidation capacity of the atmosphere and, therefore, the atmospheric budget of trace gases (Sillman et al., 1990; Seinfeld and Pandis, 2016). In this connection, studies of photochemical processes in the atmospheric boundary layer (ABL) over Siberian boreal forests are of considerable interest due to the extremely important role of high-latitude forest ecosystems in the formation of planetary sources and sinks of greenhouse and chemically active gases, including ozone (O_3), carbon monoxide (CO), and hydrocarbons (RH), including methane (CH_4) (Guenther et al., 1995; Kulmala et al., 2004; Heimann et al., 2014). At low concentrations of NO_x and high ratio RH/NO_x, which are typical tor remote areas of Northern Eurasia, the photochemical system O_3–NO_x–CO–RH is characterized by strong nonlinearity depending on NO_x concentration and general reactivity of the CO–RH mixture (Trainer et al., 1987; Sillman et al., 1990; Browne et al., 2012). This determines high sensitivity of the concentration field of ozone to regional emissions of its most important precursors—biogenic hydrocarbons and NO_x (Moiseenko et al., 2018; Thorp et al., 2020).

The available quantitative estimates of the contribution of regional biogenic and anthropogenic emissions to the tropospheric ozone balance in Siberia are partly contradictory. In particular, based on results of long-term flight measurements in the troposphere over Western and Eastern Siberia, a conclusion was made about an average downward flux of ozone from the stratosphere to the troposphere and its destruction in the surface layer in contact with the underlying surface and vegetation (Engvall-Stjernberg et al., 2012). In general, for these regions, ozone runoff in the lower troposphere dominates over its photochemical generation (Pochanart et al., 2003; Engvall-Stjernberg et al., 2012). Thus, the general trend is expressed in the decrease in the content of ozone (and other secondary oxidants) in the contaminated air mass during its advection from windward regions—ozone sources concentrated mainly in the western part of the continent (Pochanart et al., 2003; Moiseenko et al., 2018). The validity of this conclusion is confirmed by the presence of a positive vertical ozone gradient in the lower troposphere; its value in the photochemically

active period of the year (March–September) can be estimated at 5–8 ppb/km at a typical ozone concentration in the ABL of about 30–40 ppb.

The analysis of long-term O_3 and NO_x measurement data at the ZOTTO observatory (Central Siberia) with the use of back trajectory ensembles in recent papers (Moiseenko et al., 2021, 2022) indicates, however, a more complex quantitative relationship between ozone sources and sinks in the ABL as compared to the scheme described above. It was shown that photochemical ozone production during spring and summer months could occur in a wide range of NO_x concentrations typical for background and slightly contaminated (photochemically aged) air masses. According to calculations using the photostationary method, peroxide and hydroperoxide radicals are intensely accumulated under favorable meteorological conditions in the daytime (well-developed) ABL above the observatory area, which indicates processes of intense oxidation of biogenic volatile organic compounds (VOCs) and ozone production in the daytime (Moiseenko et al., 2022). Thus, the near-ground air layer in the boreal forest zone can act as a source of ozone for the ABL over remote areas of Siberia.

The conclusion about the significant role of photochemical ozone formation is also supported by data of flight observations over southern Siberia (Antokhin et al., 2013; Belan, 2010). The data show a daily increase in ozone concentration in the ABL in the period from March to September at a level of 10–15 ppb. Close values of the contribution of regional anthropogenic NO_x and VOC emissions to the surface ozone content follow from results of the numerical experiments performed using the global chemical transport model (CTM) GEOS-chem (Moiseenko et al., 2018) and the regional CTM WRF-Chem (Thorp et al., 2021). The obtained model estimates, however, need further validation using the results of comprehensive measurements of air composition in the region.

In this work, based on a series of long-term measurements of surface concentrations of O_3, NO, NO_2, and solar radiation at the regional sites (observatories) ZOTTO and Fonovaya, estimates of the photochemical ozone production rate, atmospheric lifetime of NO_x, and ozone production efficiency (OPE) per one odd nitrogen molecule during the photochemically active period of the year (March–September) are obtained. Within the framework of photochemical theory, analytical formulas establishing the dependence of these values on the NO_x concentration and reactivity of the CO–RH mixture are found for conditions of pure or slightly polluted air. The interest in such estimates is dictated by high sensitivity of the tropospheric photochemical system parameters to regional anthropogenic and biogenic emissions of ozone precursors, as well as by the strong limitation of instrumental estimates of photochemical system parameters in the ABL over boreal forests of Northern Eurasia.

1. DATA

The international observatory ZOTTO (ZOtino Tall Tower Observatory) (60°48′ N, 89°21′ E, 114 m a.s.l.) operates on the basis of the Middle Yenisei station of the Sukachev Forest Institute, Siberian Branch, Russian Academy of Sciences. The observatory is located in the taiga zone on the eastern edge of the West Siberian Plain. The nearest settlement—Zotino settlement—is 20 km to the east on the bank of the Yenisei River. The immediate vicinity of the mast is dominated by a high pine forest (*Pinus sylvestris*) with a stand height of up to 20 m. The main objective of these observations is to investigate the interaction between the atmosphere and plant biota of the boreal zone (Schulze, 2002). The measurements of near-ground concentrations of O_3, NO, and NO_2 at a height of 4 m above the ground were carried out from 2007 to 2014 using an automated instrument complex for background observations of air composition (Moiseenko et al., 2021). A detailed description of the measuring station can be found in (Heimann et al., 2014) and in other publications listed on the observatory website (www.zottoproject.org).

The Fonovaya observatory (56°25′ N, 84°04′ E, 80 m a.s.l.) is located on the right bank of the Ob River 60 km west of Tomsk and 170 km northwest of Novosibirsk in the boreal forest zone of southern taiga. A mixed forest with prevalence of birch, aspen, and pine (*Pinus sylvestris*) grows in close proximity to the site. The chemical composition and radiation parameters of the atmosphere are comprehensively monitored at the observatory in a continuous mode. A detailed description of the site and its set of devices is presented in (Antonovich et al., 2018). The work uses the measurement data on O_3, NO, NO_2 (at a height of 30 m above the ground), and integral solar radiation in 2020–2023.

The measuring devices installed at the sites underwent regular calibration and the initial data passed primary quality control in order to eliminate the artifacts caused by the occasional influence of local sources (diesel generator and motor transport, <2% of the data). With allowance for breaks due to instrument maintenance and logistics, the total observation time at ZOTTO in March–September was 1376 days (82% of the total duration of the period). The number of days of measurements at Fonovaya for the same period amounted to 835, with data filling close to 100%.

The remoteness of both observatories from large cities and industrial centers provides high sensitivity of the observational data on O_3 and NO_x to regional sources of atmospheric contamination and biogenic emissions of compounds that are ozone precursors in the areas of measurements.

Proceeding from the peculiarities of annual variations of biogenic emission intensity and conditions of atmospheric transport, data for the beginning of spring (March and April) and the vegetation period of

Table 1. Medians (lower–upper quartiles) of maximum hourly concentrations of O_3 and mean hourly concentrations of NO and NO_2 in the daytime (08:00–18:00) at the Zotino and Fonovaya stations for the spring and summer subsets of data

	O_3, ppb	NO, ppt	NO_2, ppb
March–April			
Zotino	43.3 (40.1–47.8)	20.0 (12.0–44.0)	0.89 (0.63–1.19)
Fonovaya	42.3 (38.3–47.0)	37.0 (14.0–83.0)	1.52 (1.03–2.14)
May–September			
Zotino	28.2 (22.5–35.3)	15.0 (8.0–29.0)	0.36 (0.25–0.55)
Fonovaya	31.3 (26.3–38.6)	32.0 (15.0–61.0)	0.80 (0.57–1.16)

the year (May–September) were considered separately. Hereinafter, we conventionally call them spring and summer data. The spring data characterize the air composition in the ABL during the period of the annual ozone maximum at temperate latitudes over the continent, including the areas of observatory locations. The spring maximum of ozone is determined by several large-scale factors: the increased content of ozone precursors in the lower troposphere, which is typical of the cold period; amplification of photochemical oxidation processes on the background of the seasonal increase of solar radiation; and a relatively low ozone sink to the underlying surface in the presence of snow cover (Derwent et al., 2013). The data for the summer period determine the air composition in the areas of the sites under conditions of a developed mixing layer and high biogenic VOC emissions, with an occasional influence of regional transport from the sources of atmospheric contamination—industrial areas and natural fires (Moiseenko et al., 2021). The statistics of O_3, NO, and NO_2 concentrations for the selected subsets are given in Table 1.

The calculations were performed for subsets of spring and summer data satisfying the criteria of (i) "normal" diurnal variations of ozone with a minimum between 06:00 and 08:00 and a maximum between 14:00 and 18:00 (hereinafter, LT); (ii) the total variation of hourly NO_x concentrations between 06:00 to 18:00 does not exceed 20% of the corresponding daily average concentration; and (iii) the maximum daily ozone concentration in March–April and May–September is ≥35 and 25 ppb, respectively. Fulfillment of criteria (i)–(iii) allows one to consider the quantitative estimates obtained below for the ozone production rate (P_{O_3}), NO_x lifetime (τ_N), and OPE (ΔP) as representative values for the daily surface air layer and lower ABL in a chemically homogeneous air mass under stable meteorological conditions.

2. METHODS

For each day of the analyzed period, the average rate of the increase in ozone concentration in daytime hours was calculated by the formula

$$\langle \partial [O_3]/\partial t \rangle = \Delta [O_3]_{day} / (T_2 - T_1), \quad (1)$$

where $\Delta[O_3]_{day} = [O_3](T_2) - [O_3](T_1)$, T_1 and T_2 are the times of the maximum of the measured ozone content in daytime hours (08:00–10:00) and in the afternoon (14:00–19:00), respectively (see, e.g., (Liu et al., 1987)). Hereinafter, $\langle \cdot \rangle$ denotes the mean for the period from T_1 to T_2 and [C] is concentration (mixing ratio) of the carbon compound.

When establishing the theoretical dependences of P_{O_3}, τ_N, and ΔP on $[NO_x]$, we use conclusions of the theory of photochemical ozone production under the conditions

$$[RH]/[NO_x] \gg 1, \quad [NO]/[NO_2] \ll 1, \quad [NO_x] \sim 0.2\text{–}2 \text{ ppb}, \quad (2)$$

typical for a photochemically aged air mass (with the time of air advection from main regional sources of nitrogen oxides $\geq \tau_N$) under NO_x-limiting conditions of ozone production (Sillman et al., 1990).

The rate of photochemical ozone production by the radical-chain mechanism is limited by the oxidation rate of main ozone precursors—hydrocarbons (RH) and carbon monoxide (CO)—in reactions with the hydroxyl radical OH:

$$RH + OH + O_2 \rightarrow RO_2 + H_2O, \quad (R1a)$$

$$CO + OH + O_2 \rightarrow HO_2 + CO_2, \quad (R1b)$$

where R is the hydrocarbon radical (R≡CH_3 in the case of methane) (Sillman et al., 1990; Hens et al., 2014; Lew et al., 2020). NO molecules which are present in the atmosphere interact with hydroperoxide (HO_2) and peroxide (RO_2) radicals by reactions (R2) and (R3) which finally result in accumulation of secondary VOCs (compounds of the carbonyl group, CARB) and ozone in reactions (R2)–(R6) (Trainer et al., 1987):

$$RO_2 + NO \xrightarrow{1-\alpha} NO_2 + HO_2 + CARB, \quad (R2a)$$

$$\xrightarrow{\alpha} RONO_2, \quad (R2b)$$

$$HO_2 + NO \rightarrow NO_2 + OH, \quad (R3)$$

$$NO_2 + h\nu (\lambda < 420 \text{ nm}) \rightarrow NO + O(^3P), \quad (R4)$$

$$O(^3P) + O_2 + M \rightarrow O_3 + M, \quad \text{(R5)}$$

$$O_3 + NO \rightarrow NO_2 + O_2, \quad \text{(R6)}$$

where α is the output of organic nitrates ($RONO_2$) in the reaction $RO_2 + NO$. According to the scheme presented above, OH and NO molecules are regenerated within one cycle of reactions (R1)–(R6); secondary VOCs generated by (R2a)—compounds of the carbonyl group—are subjected to further oxidation (in the reaction with OH by analogy with R1) and photodissociation with the formation of HO_2 and RO_2, which is a significant additional source of hydrogen radicals and ozone (Trainer et al., 1987; Lew et al., 2020), M is an N_2 or O_2 molecule receiving the excess of vibrational energy. The coefficient α which is equal to the number of $RONO_2$ molecules produced in one hydrogen cycle as a result of the reaction of OH with a hydrocarbon molecule (reactions R1a and R1b) tends to increase with an increase in the number of carbon atoms in the molecule and a decrease in the air temperature. In the range of atmospheric conditions, α varies from ~0 to 0.15 (Trainer et al., 1987).

The presence of NO_x molecules in the atmosphere catalyzes oxidation of CO, RH, and secondary VOCs, which is an important factor determining the length of chain (R1)–(R6) and, consequently, the magnitude of ozone production by the scheme presented above.

Far from sources of NO and NO_2 emissions, the main sink of NO_x family members occurs in reaction (R2b) and the reaction

$$OH + NO_2 + M \rightarrow HNO_3 + M. \quad \text{(R7)}$$

The forming nitric acid and organic nitrates act as intermediate reservoir compounds for NO_x. The rate of their removal from the atmosphere (in particular, in dry oxidation processes and heterophase reactions) is much higher than similar rates for NO and NO_2 (for more details, see (Sillman et al., 1990; Liebmann et al., 2019)).

In the theoretical analysis, it is convenient to use the ratio of the ozone formation rate to the rate of photochemical sink of NO_x (L_N) as a dimensionless parameter characterizing the sensitivity of the ozone field to the atmospheric content of NO_x (Trainer et al., 1993; Browne and Cohen, 2012):

$$\Delta P = \frac{P_{O_3}}{L_N} \equiv \tau_N \frac{P_{O_3}}{[NO_x]_e}, \quad (3)$$

where $\tau_N \equiv [NO_x]_e/L_N$ is the exponential lifetime of NO_x and $[NO_x]_e = P_N/L_N$ is the NO_x concentration under the assumption of local photochemical equilibrium between the sources (P_N) and sinks (L_N) of odd nitrogen. In accordance with the reaction scheme presented above, the quantity ΔP called the ozone production efficiency (OPE) (Liu et al., 1987) is numerically equal to the number of O_3 molecules produced per one NO_x molecule before its annihilation in reaction R2b or R7. In accordance with the reaction scheme presented above, for an air mixture of I hydrocarbons with concentrations $[RH]_i$, $i = 1, \ldots I$, we have

$$P_{O_3} = J_{NO_2}[NO_2] - k_{NO+O_3}[NO][O_3], \quad (4)$$

$$L_N = \alpha_{eff} k_{RO_2+NO}[RO_2][NO] + k_{OH+NO_2}[OH][NO_2], \quad (5)$$

where α_{eff} is the weighted average yield of reaction (R2b) calculated by the formula

$$\alpha_{eff} = \sum_{i=1,\ldots I} \alpha_i k_{i\text{-OH}}[RH]_i \Big/ \sum_{i=1,\ldots I} k_{i\text{-OH}}[RH]_i, \quad (6)$$

and $k_{i\text{-OH}}$ is the constant of the reaction of [OH] with the ith hydrocarbon.

According to (3)–(5), ΔP depends on time τ_N and ratio $P_{O_3}/[NO_x]_e$ which, in turn, are functions of $[NO_x]$ and other parameters of the photochemical system. The explicit form of the functional dependences $\tau_N([NO_x])$ and $\Delta P([NO_x])$ can be established within the framework of the photostationary approximation which presupposes local equilibrium between NO and NO_2 in the system of fast reactions (R2a)–(R6). Equating the photochemical sources and sinks in the corresponding balance equation for NO (reactions (R2a), (R3), (R4), and (R6)), we obtain

$$[NO]/[NO_2] = J_{NO_2}/(k_{RO_2+NO}[RO_2](1-\alpha) + k_{HO_2+NO}[HO_2] + k_{O_3+NO}[O_3]), \quad (7)$$

or

$$[NO]/[NO_2] = J_{NO_2}/(k_{OX+NO}[OX] + k_{O_3+NO}[O_3]), \quad (8)$$

where $[OX] = [HO_2] + [RO_2]$ and k_{OX+NO} is the weighted average coefficient of the reaction between NO and peroxide radicals,

$$k_{OX+NO} = k_{RO_2+NO}(1-\alpha_{eff})(1-\zeta) + k_{HO_2+NO}\zeta, \quad \zeta = [HO_2]/[OX], \quad (9)$$

Similarly, one can impose restrictions on the distribution of members of the odd nitrogen family HO_x(=OH + HO_2 + RO_2) (Sillman et al., 1990; Barket et al., 2004). Assuming that the rate of removal of the radical OH in reactions (R1a) and (R1b) is equal to the rate of its accumulation in reaction (R3), we obtain

$$[HO_2]/[OH] = Q_{RH}/(k_{HO_2+NO}[NO]), \quad (10)$$

where

$$Q_{RH} = k_{CO+OH}[CO] + k_{CH_4+OH}[CH_4] + \sum_{i=1,\ldots I-1} k_{i\text{-}OH}[RH]_i \quad (11)$$

is the general reactivity of the mixture of CO, CH_4, and [RH] with respect to OH (the contribution of the reaction of OH with CH_4 is distinguished as an individual summand).

Conclusion (10) is based on the assumption according to which the contribution of reactions (R1a) and (R1b) to the total sink of OH is prevailing as compared to the total sink in reactions of OH with NO_2 (reaction (R7)), O_3, and other compounds (for more details, see (Hens et al., 2014)). The validity of this approach is confirmed by direct quantitative estimates for the regions of the site location; the estimates show an insignificant contribution of the reactions OH + O_3 and OH + NO_2 (of the sum $k_{OH+O_3}[O_3] + k_{OH+NO_2}[NO_2]$) as compared to the quantity Q_{RH} (11) (see the discussion in Subsection 3.3). In contrast to OH, the corresponding balance equations for peroxide radicals include second order reactions between members of the HO_x family. The reactions, along with the reaction of HO_2 with isoprene, provide the main contribution to the sink of members of the odd nitrogen family under conditions (2) (Hens et al., 2014). In the absence of instrumentation data allowing one to independently estimate the RO_2 and HO_2 concentrations, we below use a constant quantity $\zeta = 1/3$ which agrees with data of direct measurements of the peroxide radical content in forests of temperate and high latitudes (Hens et al., 2014; Lew et al., 2020).

Using expressions (8) and (10), we reduce (5) to the form

$$L_N = P_{O_3}\left(\alpha(1-\zeta)k' + k_{OH+NO_2}[NO_2]\zeta k''/Q_{RH}\right), \quad (12)$$

($k' = k_{RO_2+NO}/k_{OX+NO}$, $k'' = k_{HO_2+NO}/k_{OX+NO}$). When carrying out the calculations, we can put with sufficient accuracy for practical purposes $k' = k'' = 1$ and $[NO_2] \approx [NO_x]$, whence with allowance for (3) we obtain

$$\tau_N \equiv [NO_x]/L_N = \frac{[NO_x]\cdot\Delta P}{P_{O_3}}, \quad (13)$$

$$\Delta P = 1/\left[\alpha_{eff}(1-\zeta) + k_{OH+NO_2}[NO_x]\cdot\zeta/Q_{RH}\right]. \quad (14)$$

Formulas (13) and (14) establish the explicit form of the dependences of τ_N and ΔP on concentration of NO_x and ozone production rate P_{O_3} (4) at given external parameters ζ, α_{eff}, and Q_{RH}. In calculations of P_{O_3}, the NO_2 photodissociation rate in the absence of clouds was estimated by the technique used in the recent work (Moiseenko et al., 2022). The obtained quantity ($J^*_{NO_2}$) was then recalculated taking into account the correction for clouds based on measurements of global solar radiation by the formula

$$J_{NO_2}(\text{in the presence of clouds}) = J^*_{NO_2}(G_{obs}/G^*), \quad (15)$$

where G_{obs} and G^* are the measured solar radiation fluxes in the presence of clouds and clear sky, respectively (Kleinman et al., 1995). The rate constants were taken from (Atkinson et al., 2004, 2006). The yield constants α_i are presented in (Browne et al., 2013).

3. RESULTS

3.1. Diurnal Variations of O_3, NO, and NO_2

At the level of seasonal statistics, the surface concentrations of O_3, NO, and NO_2 are characterized by a stable unimodal diurnal variation (Fig. 1) the dynamics of which is controlled by changes in the height of the mixing layer and intensity of photochemical processes. The amplitude of the mean daily ozone variations (the difference between the maximum in the daytime and minimum in the morning hours) naturally increases from spring to summer, being equal to about 8 ppb at Fonovaya and 5 ppb at ZOTTO in April and about 10 ppb at both stations in July. The decrease in ozone in the period from 20:00 to 08:00 is caused by its uncompensated sink to the underlying surface and vegetation during the period of establishment of the temperature inversion preventing the air exchange between the surface layer and the overlying air layers. An additional contribution to the nocturnal decrease in ozone can be provided by ozonolysis reactions of VOCs; among them, the most significant one is the reaction of O_3 with monoterpenes providing the ozone decrease at a level of 0.1 ppb/h under conditions of coniferous vegetation dominance (Moiseenko et al., 2022). In April, the nocturnal ozone decrease at ZOTTO is much weaker due to the persisting snow cover and comparatively lower dry deposition rates as compared to regions of southern Siberia.

In addition to differences in the seasonal dynamics of vegetation and snow cover, the observed systematic differences between nocturnal ozone concentrations at both stations can be determined by local factors. The ZOTTO observatory is located at the top of a slightly sloping hill dominating over the surrounding waterlogged hollows, while Fonovaya is located in the Ob River valley in close proximity to the river channel, which manifests itself in a comparatively more powerful layer of nocturnal inversion the locking effect of which is more pronounced.

The maximum of the diurnal variations of ozone falls in the afternoon or late in the afternoon (14:00–20:00) (Figs. 1a and 1b), when the rate of its photochemical production is equalized by destruction in chemical reactions, vertical turbulent transport, and sink to the underlying surface. The closeness of the ozone concentration dynamics at both stations in daytime hours, both in spring and summer months, indicates the regional nature of the diurnal maximum not

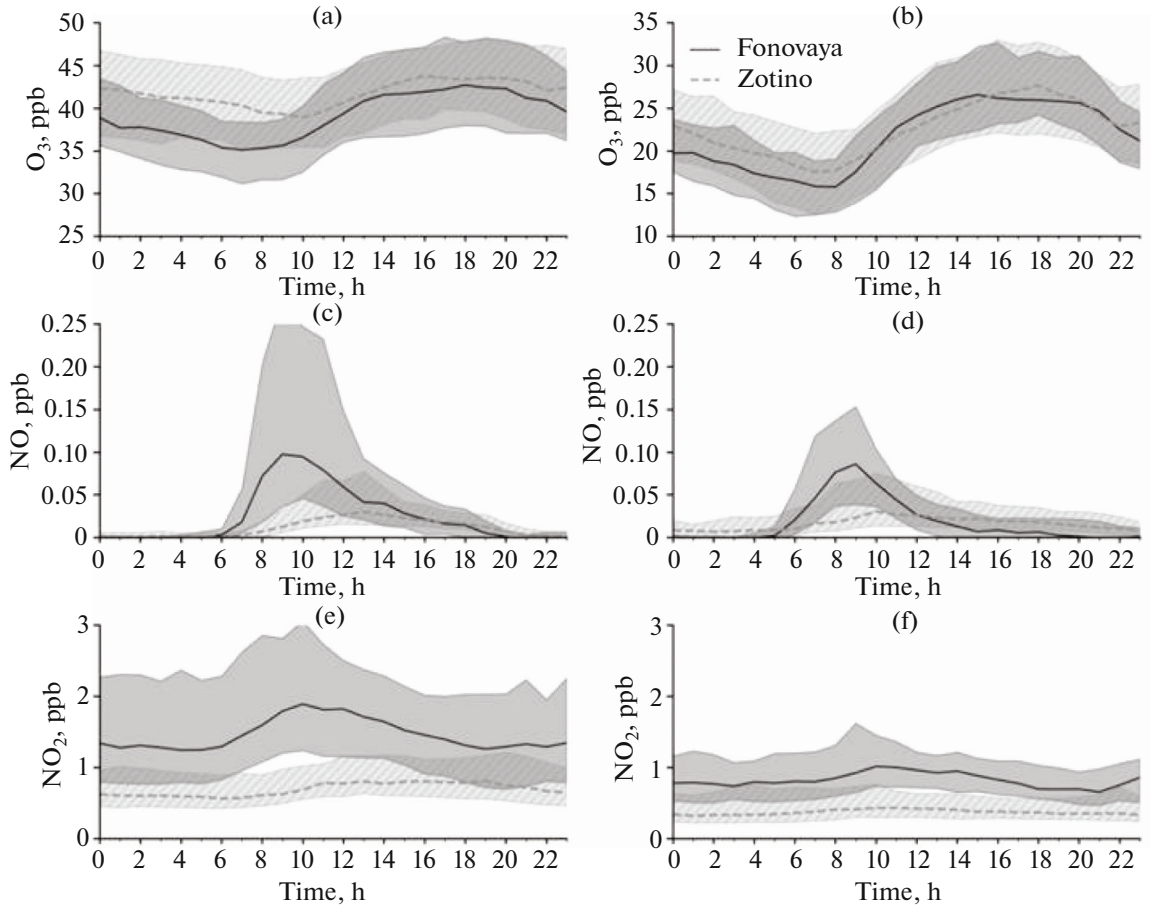

Fig. 1. Daily variations of (a, b) O_3, (c, d) NO, and (e, f) NO_2 in (a, c, e) April and (b, d, f) July at the Zotino (2007–2014) and Fonovaya (2020–2023) stations. Medians and upper and lower quartiles of mean hourly concentrations.

connected with peculiarities of the station location. The magnitude of the diurnal maximum is controlled by meteorological factors and the chemical background of the air mass, including the concentration of nitrogen oxides (see Subsection 3.2).

The annual variations of NO_x at the stations are unimodal, by analogy with the tropospheric content of other compounds—ozone precursors, with a maximum in winter and a minimum in summer months. The medians of daily mean NO_x concentrations at Fonovaya (at ZOTTO) are 1.5 (0.75) ppb in April and 0.9 (0.45) ppb in July. In general, the air in the site areas is characterized by low (<0.05) ratio $[NO]/[NO_2]$, typical of remote areas with low anthropogenic load (Bakwin et al., 1994). With allowance for (7), this feature can be explained by the reaction of NO with peroxide radicals formed during oxidation of biogenic hydrocarbons. The final effect of this reaction is a redistribution among members of the odd nitrogen family towards higher concentrations of NO_2 under conditions of the generally low content of NO_x.

The diurnal NO maximum at Fonovaya in both spring and summer months is observed at around 9 a.m., when the ratio $[NO]/[NO_2]$ also reaches the highest value (~0.05) (Figs. 1c and 1d). The similar maximum at ZOTTO is shifted to later hours (13:00 in April and 10:00 in July), which can be explained, in part, by lower UV radiation fluxes and photodissociation rates of nocturnal reservoir nitrogen compounds (the ZOTTO observatory is located 4° north of Fonovaya). In the following hours, the NO concentration monotonically decreases as a result of the increase in the concentration of peroxide radicals and the shift of equilibrium toward NO_2; in the evening, due to the decrease in solar UV radiation and photodissociation rate of NO_2.

It should be noted, however, that the redistribution between NO and NO_2 throughout the day cannot explain the observed diurnal variations of NO_2 the amplitude of which is several times greater than the similar value for NO both in spring and summer months (Figs. 1e and 1f). The presence of a pronounced diurnal maximum of NO_2 in the morning hours can be explained by the involvement of overlying air during the period of morning rise of the ABL height in the presence of a positive vertical gradient of

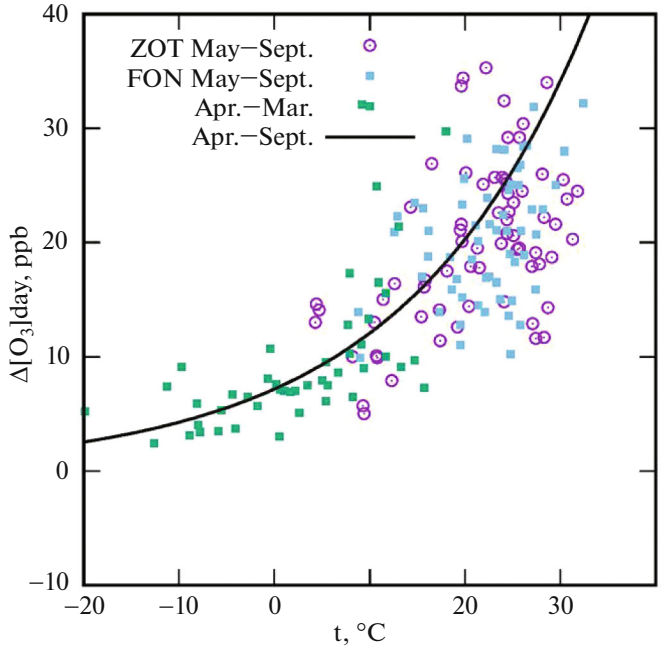

Fig. 2. Dependence of $\Delta[O_3]_{day}$ on the maximum daytime air temperature. The solid line shows fitting to spring and summer data by formula (13).

reactive nitrogen (NO_y = NO_x + reservoir compounds) at heights of the lower troposphere. Thus, a likely source of high NO_2 concentrations in the morning hours is the partial photodissociation of reservoir nitrogen compounds in the growing ABL. In absolute numbers, this effect is most pronounced in March–April on the background of the general increased content of NO_y in the continental ABL as compared to summer months. The observed monotonic decrease in NO_2 during the daytime hours is most likely photochemical in nature and is related to the formation of organic nitrates in the reaction (R8); thus, the surface air layer provides the sink of NO_y the main source of which in the site area is air advection from regions with high anthropogenic emissions (Moiseenko et al., 2021). In summer months, the amplitude of daily variations and absolute concentrations of NO_2 are approximately two times lower as compared to the same values in March–April, which indicates the absence of significant surface sources of NO_x, including biogenic ones, in the vicinity of the sites. The role of regional transport in the formation of increased NO_x concentrations in the site areas during this period of the year is also reduced due to a decrease in the photochemical lifetime of odd nitrogen (see below).

The consistency manifesting itself between the observational data at both sites, among other things, in practically identical daily ozone variations and NO_x source regions (Moiseenko et al., 2021) indicates the closeness of main factors controlling the ozone content in the ABL over the measurement areas. This circumstance allows one to consider data series at the Fonovaya and ZOTTO in a common context when investigating photochemical processes in the troposphere above boreal forests of Siberia. The quantitative estimates presented below for spring and summer months were obtained on the basis of the combined data subsets at both sites. In the final presentation of the results, the points in Figs. 2–4 are divided into three groups based on the corresponding variability ranges of NO_x concentrations: (1) summer data from Fonovaya; (2) summer data from Zotino; and (3) spring data from both stations. Distinguishing of data groups (1) and (2) allows one to illustrate the universal character of the dependence of OPE and other quantities in a relatively wider range of $[NO_x]$ as compared to similar variability ranges at each station due to the differences in their remoteness from the main regional sources of anthropogenic emissions. At the same time, combining the spring data subsets into one group seems to be acceptable due to similar variability ranges of measured NO_x concentrations. The latter circumstance is dictated by a comparatively greater homogeneity of the air composition in the region under study in the cold season, with a comparatively smaller role of local biogenic sources of gases—ozone precursors, as compared to the summer period.

3.2. Dependence of Daytime Accumulation of Ozone on Air Temperature

In general, a statistically significant positive correlation between photochemical production of ozone

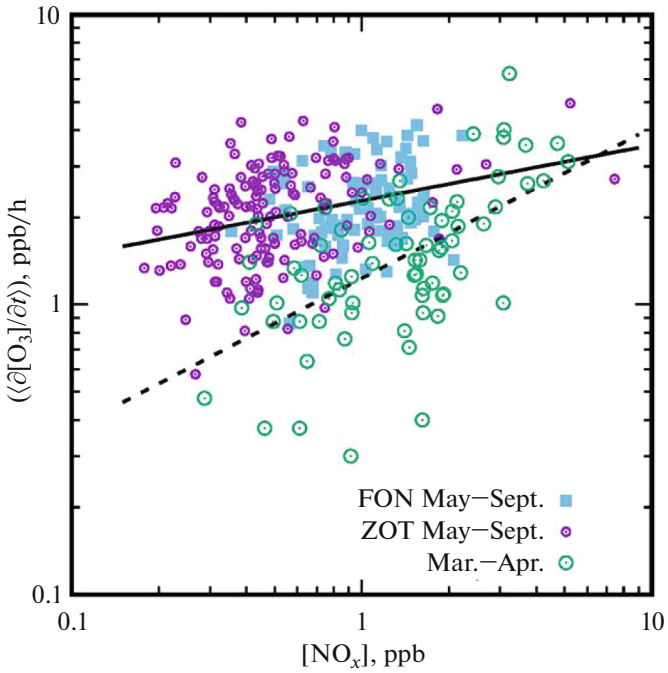

Fig. 3. Dependence of the average rate of the increase in daytime ozone concentration ($\langle\partial[O_3]/\partial t\rangle$) (1) on $[NO_x]$. The solid (dashed) line shows fitting to summer (spring) data by formula (17).

in diurnal hours $\Delta[O_3]_{day}$ (1) and air temperature (t, °C) takes place at both sites for the spring–summer period (Fig. 2). The data presented in the figure for the combined subset of spring and summer values can be approximated by the function

$$\Delta[O_3]_{day}(t) = A\exp[B(t-15°C)], \qquad (16)$$

where $A = 15.7 \pm 1.06$, $B = 0.052 \pm 0.004$ ($R^2 = 0.50$) in the range of t from −20 to +35°C (hereinafter, the presented values for the regression coefficients are everywhere mean expected ±2 standard deviations). As follows from the figure, the quantity $\Delta[O_3]_{day}$ increases with air temperature; at the same time, the slope of the curve increases with increasing temperature, which can be explained by the nonlinear increase in OPE (and biogenic NO emissions) with increasing daytime air temperature, especially in hot weather (>20°C) on the background of high solar insolation (Belan et al., 2017). The considerable scatter of experimental points relative to the average trend, however, indicates a large role of other factors, including the dependence of OPE on the chemical composition of the air mass (see Subsection 3.3), which determines the ozone production rate under specific daytime conditions.

Within the framework of dependence (16) established above, the sensitivity to temperature determined by parameter B and the coefficient of determination for the summer subset turn out to be noticeably higher as compared to the similar values in March–April, probably due to a comparatively greater influence of local (biogenic) VOC emissions in the site areas on ozone formation in the warm period of the year.

The exponential character of the dependence of daily ozone accumulation on air temperature was established earlier in (Belan et al., 2017) for the TOR station of the Institute of Atmospheric Optics in the suburbs of Tomsk. The station is located in a forest zone, with no significant sources of anthropogenic contamination, which allows one to compare the results obtained by the authors with the estimates presented above. In (Belan et al., 2017), the temperature effect in the ozone content was estimated by the increment of maximum daily ozone concentrations for periods with a steady increase or decrease in air temperature during the change of air masses (according to the authors' terminology, heat and cold waves). The average increase in ozone concentration with an increase in temperature by 1°C at the TOR station in individual years amounted to 0.7–2.5 ppb/1°C at t = 0°C and 1.2–5 ppb/1°C at t = 20°C. A similar value calculated using formula (16) (the product $B\cdot\Delta[O_3]_{day}$) amounts to 0.37 ppb/1°C at t = 0°C and 1.05 ppb/1°C at t = 20°C. The temperature effect in the measured ozone concentrations at the Fonovaya and ZOTTO sites thus appears to be noticeably lower than at the TOR station, especially in the beginning of spring on the background of relatively low air temperatures. This difference can be explained by the relatively lower NO_x content at the regional stations (~0.5–1 ppb) as compared to $[NO_x]$ ~ 3–4 ppb at the TOR station (Belan et al., 1998). Under the conditions of the previously established NO_x-limiting regime of ozone production in the ABL over Siberia (Moiseenko et al., 2022), the rate of photochemical ozone production decreases with and increase in the NO_x concentration, which

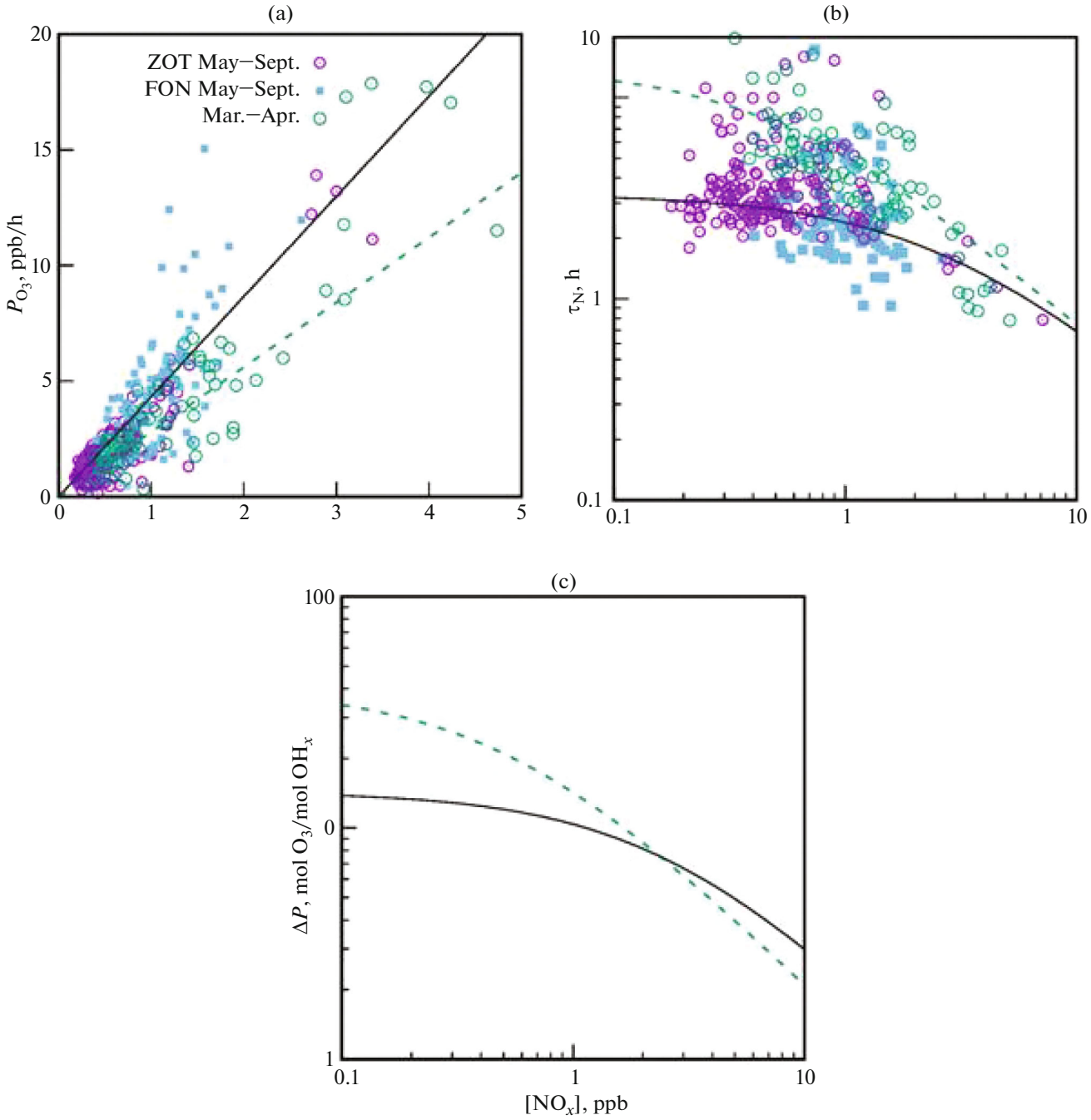

Fig. 4. Dependences of P_{O_3} (4), τ_N (13), and ΔP (14) on [NO_x]. The solid (dashed) line in figures (a), (b), and (c) show calculations by formulas (18), (19), and (14), respectively, for subsets of summer (spring) data.

just determines a relatively higher sensitivity of the surface ozone concentration to temperature-dependent emissions of biogenic VOCs at the TOR station.

3.3. Effect of Nitrogen Oxides on Photochemical Production of Ozone

According to Fig. 3, the rate of daily accumulation of ozone in the ABL, $\langle \partial[O_3]/\partial t \rangle$ (1), increases with an increase in the mean daily concentration of NO_x. The relationship between these quantities can be approximately expressed by means of an empirical formula

$$\langle \partial[O_3]/\partial t \rangle = A \cdot [NO_x]^B, \quad (17)$$

where $A = 1.11 \pm 0.18$, $B = 0.71 \pm 0.20$ ($R^2 = 0.36$) and $A = 2.44 \pm 0.16$, $B = 0.50 \pm 0.08$ ($R^2 = 0.14$) for the spring and summer subsets, respectively. In accordance with the presented expression, the derivative $\partial(\langle \partial[O_3]/\partial t \rangle)/\partial[NO_x]$ at $B < 1$ decreases with an

increase in $[NO_x]$. Therefore, the quantity $\langle \partial[O_3]/\partial t \rangle$ increases more slowly at high concentrations of NO_x, which can be explained by the decrease in ozone production efficiency with an increase in the atmospheric content of nitrogen oxides (Liu et al., 1987; Sillman et al., 1990; Trainer et al., 1993; Browne and Cohen, 2012). The rate of ozone production in May–September turns out to be about twice as high as compared to the same value in March–April, in line with the general tendency of the increase in $\Delta[O_3]_{day}$ with the increase in air temperature (Fig. 1).

The experimental point scatter observed in Fig. 3 is caused by the wide range of conditions for ozone production in the surface layer in individual days depending on specific meteorological conditions and the photochemical prehistory of the air mass. In general, however, for the $[NO_x]$ interval under consideration, a steady trend toward a decrease in the rate of ozone production with an increase in $[NO_x]$ per molecule of odd nitrogen (i.e., the ratio $\langle \partial[O_3]/\partial t \rangle / [NO_x]$) takes place, in accordance with general properties of the atmospheric photochemical system.

The experimental data presented in Fig. 4a are consistent with conclusions of the photochemical theory (Sillman et al., 1990) which establish a linear dependence of the in situ ozone generation rate (P_{O_3}) on the concentration $[NO_x]$ in clean/slightly polluted air. The corresponding empirical dependence obtained by fitting to spring ($R^2 = 0.34$) and summer ($R^2 = 0.87$) data subsets has the form

$$P_{O_3} = A' \cdot [NO_x] + B', \quad (18)$$

where $A' = 2.8 \pm 0.6$ (4.33 ± 0.2), $B' = -0.39 \pm 1.11$ (-0.19 ± 0.18) for the spring (summer) subset. Comparing Figs. 3 and 4a, we come to a conclusion that the value of P_{O_3} in the $[NO_x]$ range from 0.3 to 3 ppb exceeds the observed growth rate of ozone concentration in the surface layer ($\langle \partial[O_3]/\partial t \rangle$) by a factor of 1.5–4; this difference increases with the increasing NO_x concentration. In accordance with the results (Moiseenko et al., 2022), the rate of ozone sink to the underlying surface and in reactions with other compounds on photochemically active days turns out to be significantly lower than the rate of ozone accumulation due to reactions (R1)–(R6). Thus, neglect of ozone sink during the daytime cannot cause the observed discrepancy between the theoretical and experimental estimates. This contradiction is eliminated by introducing the assumption of a significant contribution of vertical turbulent exchange to the ozone balance in the range of ABL heights (Belan et al., 2010). According to calculations (Trainer et al., 1987) and measurement data (Spirig et al., 2004; Petersen et al., 2023), the concentration of biogenic hydrocarbons decreases rapidly with height in the layer with a thickness of the first hundreds of meters, which indicates the predominant course of oxidation processes and accompanying ozone production in the lower part of the ABL. Therefore, the surface air layer serves as an ozone source for the daytime ABL, in agreement with results of (Moiseenko et al., 2022). However, the validity of our proposed explanation needs additional verification with the use of experimental data allowing one to directly estimate the ozone generation rate in the range of lower tropospheric heights.

The instrumental estimates of the NO_x lifetime obtained by formula (13) are presented in Fig. 4b. The lines in the figure show fitting by the approximate formula

$$\tau_N \approx \Delta P / A', \quad (19)$$

which is obtained by substitution of (18) into (13) with allowance for smallness of the contribution of the free term B' in calculations of the quantity P_{O_3}.

The calculations were performed at $Q_{RH} = 2.28\ s^{-1}$ ($3.91\ s^{-1}$) and $\alpha_{eff} = 0.037$ (0.105) the spring (summer) subset with the use of the empirical values of P_{O_3} presented in Fig. 4a. The parameters Q_{RH} and α_{eff} were specified using mean seasonal concentrations $[CH_4]$ = 1950 (2000) ppb, [CO] = 220 (100) ppb, [IZO] = 0.05 (0.7) ppb, [TERP] = 0.2 (0.6) ppb, and [AR] = 0.90 (0.45) ppb for spring (summer) subsets, where IZO, TERP, and AR mean isoprene, monoterpenes, and aromatic hydrocarbons (xylene, benzene, and toluene), respectively. The values of the coefficient α are 0.001 (CH4), 0.029 (BENZ), 0.08 (TOL), XYL (0.081), 0.117 (IZO), and 0.18 (TERP) (Browne et al., 2013). The accepted mean concentrations of CH_4 and CO were calculated directly from the site measurements. Concentrations of biogenic (IZO, TERP) and anthropogenic (AR) hydrocarbons typical for the summer season were specified using the proton mass spectrometer data of the TROICA-12 expedition (Moscow–Vladivostok–Moscow) in summer 2008 (Fig. 5). The total time of measurements during the forward and backward passes was about 12 days about a quarter of which falls on anticyclonic conditions characterized by low wind speeds and maximum daily air temperatures of 27–32°C (a subset of measurements from the upper quartile in Fig. 5). These meteorological conditions correspond to "normal" diurnal variations of O_3, IZO, and TER (with a daytime maximum of ozone and isoprene and a nighttime maximum of monoterpenes) which we consider as representative also for the areas of the measuring sites taking into account the data selection criteria we used (see Subsection 2.1). The summer values of IZO, TERP, and AR presented above correspond to mean concentrations on a section of the Trans-Siberian railroad from Novosibirsk to Krasnoyarsk beyond populated areas.

The subset of TROICA-12 data from the lower quartile of air temperatures (Fig. 5) falls on the period of unstable weather conditions in Siberia and the

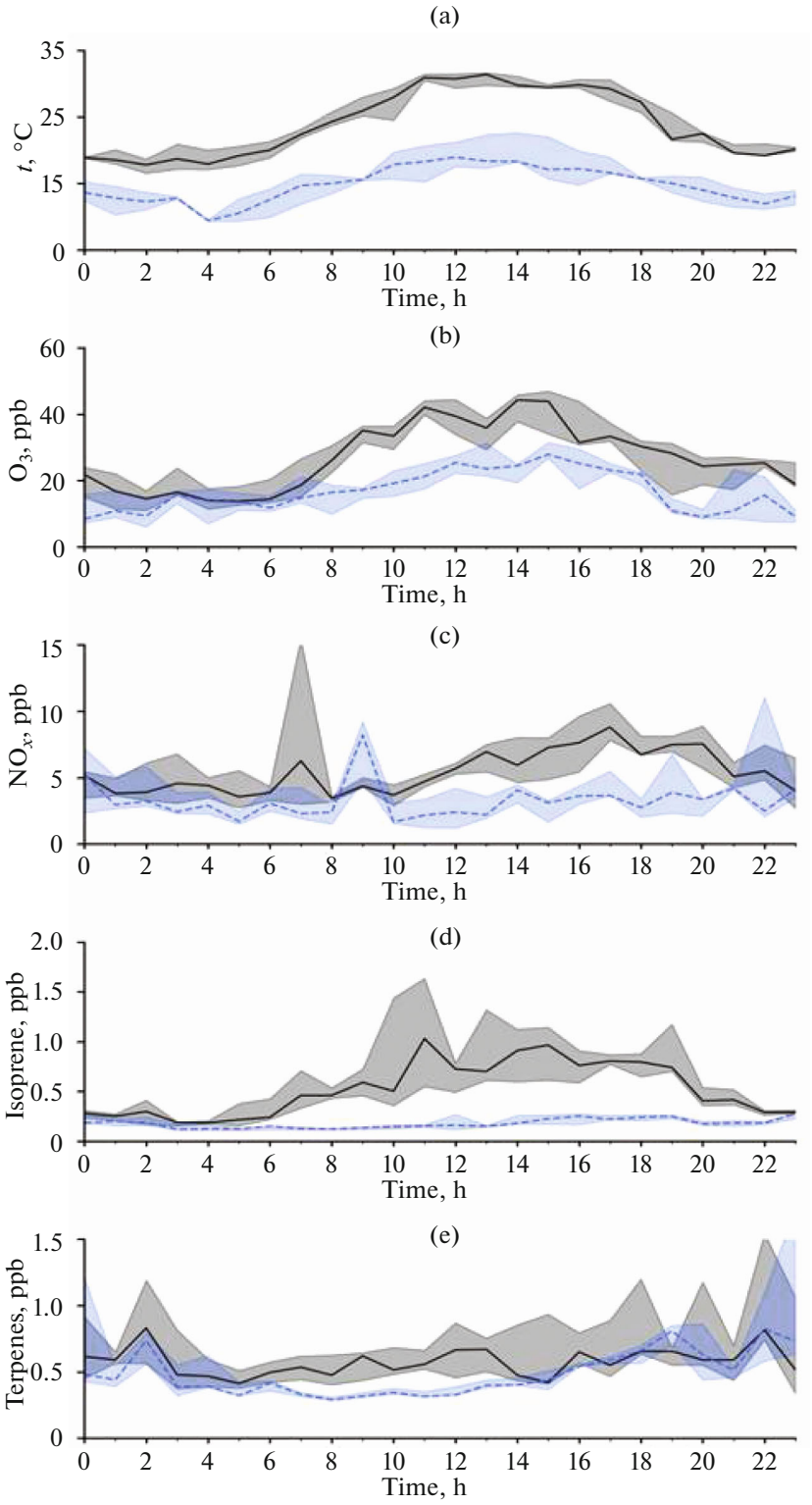

Fig. 5. Daily variations in t, O_3, NO_x, isoprene, and monoterpenes along the Trans-Siberian Railway in the TROICA-12 expedition. Statistics for data subsets from the upper and lower quartiles of mean air temperatures for each hour: median (the solid line), upper and lower quartile of the quantities in the given subset (painting). Local time is plotted on the abscissa axis.

European territory due to frontal activity. This period was characterized by cool and rainy weather, absence of a pronounced diurnal variation of impurities, and comparatively lower concentrations of ozone and isoprene. The data presented in Fig. 5 show a strong dependence of the surface ozone and isoprene content on air temperature, while for monoterpenes the trend is much weaker (Young et al., 1997; Hakola et al., 2009). In the absence of direct data for the area under study, the March–April concentrations of isoprene and monoterpenes (0.05 and 0.5 ppb, respectively) used for calculation of Q_{RH} were obtained by linear extrapolation of the corresponding temperature dependences following from the TROICA data to the average temperature of +2.5°C for the ZOTTO and Fonovaya regions during this period of the year (see Fig. 2a). The spring concentrations of aromatic compounds the emissions of which are mainly anthropogenic in nature (Taraborrelli et al., 2021) were taken to be twice as high as summer concentrations based on the ratio of spring and summer CO concentrations.

The individual contributions of the abovementioned impurities to the total reactivity obtained by multiplying the impurity concentration by the constant of the reaction with hydroxyl ($k_{i\text{-OH}}[RH]_i$, dimension s^{-1}) are presented below:

	CH_4	CO	IZO	TERP	AR	Q_{RH}	Q'_{RH}
Spring	0.21	1.45	0.14	0.31	0.17	2.28	0.55
Summer	0.22	0.66	2.03	0.92	0.08	3.91	0.25

The last column of the table presents values of the "additional" reactivity Q'_{RH} ($= k_{OH+O_3}[O_3] + k_{OH+NO_2}[NO_2]$) caused by reactions of hydroxyl with O_3 and NO_2. One can see that the condition $Q'_{RH} \ll Q_{RH}$ used in the derivation of (10) is fulfilled with high accuracy in summer months under the conditions of predominance of local biogenic emissions in the areas of the sites. In spring months, the relative contribution of Q'_{RH} is noticeably higher in view of higher concentrations of ozone and nitrogen oxides and lower concentrations of biogenic hydrocarbons; however, even in this case, the contribution of Q'_{RH} to the total hydroxyl sink can be neglected with sufficient accuracy for practical estimates.

In the absence of detailed data on the composition of VOCs, taking into account the five abovementioned compounds allows one to obtain a lower estimate of the real value of Q_{RH}. However, it should be noted that the contributions of primary biogenic compounds we take into account—isoprene and monoterpenes—make a determining contribution to the total reactivity of biogenic hydrocarbons. In particular, taking into account the reaction of hydroxyl with methyl vinyl ketone and methacrolein formed in the process of isoprene oxidation leads to an increase in Q_{RH} only by 1–3% in view of the significantly smaller constants of reactions with hydroxyl as compared to the constant of the reaction OH + IZO and the general low concentrations of isoprene oxidation products (<1–2 ppb) established during the TROICA-12 expedition. A similar conclusion can be made regarding hydrocarbons the main atmospheric source of which is anthropogenic emissions. As follows from the estimates presented above, the contribution of aromatic compounds to the calculated Q_{RH} does not exceed 1.5%. Taking into account the significant fraction of aromatic compounds in regional anthropogenic VOC emissions (Skorokhod et al., 2017; Berezina et al., 2017) which is numbered in the first tens of percent, it can be assumed that the contribution of the latter to the total reactivity of photochemically aged air will be low as compared to the contribution of local emissions of primary biogenic hydrocarbons.

From the numerical estimates presented above, the relatively small variation of *average* values of Q_{RH} from spring to summer also becomes clear. The maximum of surface concentrations of biogenic hydrocarbons occurs in summer, when the CO content reaches its annual minimum, while in the cold season the opposite trend takes place; as a consequence, the total reactivity of the mixture varies little from season to season, despite significant variations in the individual contributions under consideration.

The strong dependence of the odd nitrogen lifetime on the composition of the reactive mixture and NO_x concentration (Fig. 5b) which was confirmed by our calculations and represents an important feature of the photochemistry of the lower troposphere has been emphasized in a large number of papers (Liu et al., 1987; Browne and Cohen, 2012; Kenagy et al., 2018). The theoretical and experimental estimates of τ_N obtained by different authors vary within a wide range, including due to differences in the photochemical age of the air mass. At NO_x concentrations of 0.4–1 ppb typical for the site areas, the range of variations τ_N we calculated is 1.5–4 h, which is in agreement with earlier estimates (Browne and Cohen, 2012) of τ_N (3–5 h) for the ABL over boreal forests of Canada during summer months at $[NO_x] < 0.5$ ppb. The estimate for τ_N we obtained for March–April (~9 h) is within the range of exponential NO_x lifetimes in the daytime (6.3 h) and nighttime (29 h) during the cold season; these lifetimes were established in (Kenagy et al., 2018).

The dependence of OPE on $[NO_x]$ calculated by formula (14) under the abovementioned average seasonal values of Q_{RH} and α_{eff} is presented in Fig. 4c. The medians of the measured NO_x concentrations at ZOTTO (see Table 1) are in correspondence with the OPE values of ~15.3 (12.6) mol O_3/mol NO_x for the spring and summer subsets of measurements, respectively. The similar value at Fonovaya in spring and

summer months is about 11 mol O_3/mol NO_x. The presented values can be considered as representative for the surface air layer in boreal forests on photochemically active days of the spring–summer period.

In accordance with the general form of expression (14), the contribution of the OH + NO_2 reaction to the total odd nitrogen effluent increases with increasing NO_x concentration. The critical NO_x concentration separating the $RONO_2$- and HNO_3-limiting regimes of odd-nitrogen sink can be estimated from the expression

$$[NO_x]_c = \frac{Q_{RH}\alpha_{eff}(1-\varsigma)}{k_{OH+NO_2}\cdot\varsigma}. \quad (20)$$

The value of $[NO_x]_c$ for the spring and summer data subsets amounts to 0.55 and 2.63 ppb, respectively. Using (20), let us write formula (14) in the form most convenient for the analysis:

$$\Delta P = \frac{1}{\alpha_{eff}(1-\varsigma)}\frac{1}{1+[NO_x]/[NO_x]_c}. \quad (21)$$

According to (19) and (21), $\tau_N \sim \Delta P \sim [\alpha_{eff}(1-\zeta)]^{-1}$ at $[NO_x] \ll [NO_x]_c$ ($RONO_2$-limiting regime). According to Fig. 5c, this asymptotical behavior is in correspondence with the values ΔP = 12 (32) mol O_3/mol NO_x; at the same time, in the range of main variability of NO_x concentrations in summer months (0.2–2 ppb), by virtue of fulfillment of the condition $[NO_x] < [NO_x]_c$, a weak dependence of OPE on the NO_x content takes place. At $[NO_x] \gg [NO_x]_c$, $\tau_N \sim \Delta P \sim [NO_x]^{-1}$, which determines the strong dependence of the quantities τ_N and OPE on the NO_x concentration under conditions of HNO_3-limiting regime of odd nitrogen sink both in spring and in summer months.

CONCLUSIONS

Forest ecosystems of Northern Eurasia are among the climatically significant sources of hydrocarbons and their oxidation products (secondary VOCs and CO) that form an increased level of concentrations of ozone precursors in the continental boundary layer. Photodissociation of ozone and other secondary compounds formed in the process of oxidation of primary biogenic hydrocarbons by the radical–chain mechanism with the participation of the odd nitrogen family as a catalyst is a significant source of hydroxyl in the troposphere the content of which determines the lifetime of chemically active and greenhouse gases. Correct accounting of the balance of ozone and odd nitrogen is, therefore, the most important part of the research on the response of the tropospheric photochemical system to the climatic trends of natural and anthropogenic emissions.

Results of this work confirm the previously formulated conclusion about the key role of regional emissions of nitrogen oxides in photochemical ozone production in the ABL over boreal forests of central and southern Siberia—regions traditionally classified as ecologically clean. This influence is traced in the experimental data obtained at the regional stations ZOTTO and Fonovaya based on the corresponding correlations between the ozone content, air temperature, and NO_x concentration; spatial localization of ozone source regions using inverse modeling methods (Moiseenko et al., 2021); and direct instrumental estimates of photochemical parameters of the surface layer in the areas of the measuring sites. According to the results obtained, the surface air layer in boreal forests during the photochemically active period of the year can act as a source of ozone for the daytime ABL. Organic peroxide radicals formed in the process of oxidation play a dual role in this process. On the one hand, they participate in the photochemical ozone production (in the reaction of HO_2 with NO); on the other hand, they reduce the efficiency of ozone production through reactions leading to NO_x sink in the formation of organic nitrates. The total effect of the abovementioned differently directed processes strongly depends on the composition of the air mixture and the ratio RH/NO_x. The strong dependence of OPE and odd nitrogen lifetime on the NO_x content under conditions of a moderately contaminated ABL ($[NO_x] \geq 1$–2 ppb) established in this work makes the problem of controlling regional anthropogenic emissions of nitrogen oxides as part of the general problem of minimizing the risks associated with air contamination from natural and anthropogenic sources topical.

FUNDING

This study was supported by the Russian Science Foundation, project no. 20-17-00200 (calculations and analysis of the results). Experimental data on the ZOTTO observatory were prepared within the framework of the state assignment no. 1021042900488-7-1.5.10 for the Institute of Atmospheric Physics. Experimental data on the Fonovaya observatory were collected and prepared within the framework of the state assignment no. 121031500342-0 for the Institute of Atmospheric Optics.

CONFLICT OF INTEREST

The authors of this work declare that they have no conflicts of interest.

REFERENCES

Antokhin, P.N., Arshinova, V.G., Arshinov, M.Yu., Belan, B.D., Belan, S.B., Davydov, D.K., Kozlov, A.B., Krasnov, O.A., Praslova, O.V., Rasskazchikova, T.M., Savkin, D.E., Tolmachev, G.N., and Fofonov, A.V., Diurnal dynamics of the vertical ozone distribution in the atmospheric boundary layer in the Tomsk area, *Opt. Atmos. Okeana*, 2013, vol. 26, no. 8, pp. 665–672.

Antonovich, V.V., Antokhin, P.N., Arshinov, M.Yu., Belan, B.D., Balin, Yu.S., Davydov, D.K., Ivlev, G.A., Kozlov, A.V., Kozlov, V.S., Kokhanenko, G.P., Novoselov, M.M., Panchenko, M.V., Penner, I.E., Pestunov, D.A., Savkin, D.E., et al., Station for the comprehensive monitoring of the atmosphere at Fonovaya Observatory, West Siberia: Current status and future needs, *Proc. SPIE-Int. Soc. Opt. Eng.*, 2018, vol. 10833, p. 10833Z.

Atkinson, R., Baulch, D.L., Cox, R.A., Crowley, J.N., Hampson, R.F., Hynes, R.G., Jenkin, M.E., Rossi, M.J., and Troe, J., Evaluated kinetic and photochemical data for atmospheric chemistry: Volume I. Gas phase reactions of Ox, HOx, NOx and SOx species, *Atmos. Chem. Phys.*, 2004, vol. 4, pp. 1461–1738. https://doi.org/10.5194/acp-4-1461-2004

Atkinson, R., Baulch, D.L., Cox, R.A., Crowley, J.N., Hampson, R.F., Hynes, R.G., Jenkin, M.E., Rossi, M.J., and Troe, J., IUPAC subcommittee: Evaluated kinetic and photochemical data for atmospheric chemistry: Volume II. Gas phase reactions of organic species, *Atmos. Chem. Phys.*, 2006, vol. 6, pp. 3625–4055. https://doi.org/10.5194/acp-6-3625-2006

Bakwin, P.S., Jacob, D.J., Wofsy, S.C., Munger, J.W., Daube, B.C., Bradshaw, J.D., Sandholm, S.T., Talbot, R.W., Singh, H.B., and Gregory, G.L., Reactive nitrogen oxides and ozone above a taiga woodland, *J. Geophys. Res.*, 1994, vol. 99, no. D1, pp. 1927–1936. https://doi.org/doi:10.1029/93JD02292.

Barket, D.J. Jr., Grossenbacher, J.W., Hurst, J.M., Shepson, P.B., Olszyna, K., Thornberry, T., Carroll, M.A., Roberts, J., Stroud, C., Bottenheim, J., and Biesenthal, T., A study of the NOx dependence of isoprene oxidation, *J. Geophys. Res.*, 2004, vol. 109, p. D11310. https://doi.org/10.1029/2003JD003965

Belan, B.D., Kovalevskii, V.K., Plotnikov, A.P., and Sklyadneva, T.K., Temporal dynamics of ozone and nitrogen oxides in the surface layer of the Tomsk area, *Opt. Atmos. Okeana*, 1998, vol. 11, no. 12, pp. 1325–1327.

Belan, B.D., Tolmachev, G.N., Fofonov, A.V., Ozone vertical distribution in the troposphere over south regions of Western Siberia, *Atmos. Ocean. Opt.*, 2011, vol. 24, no. 2, pp. 181–187.

Belan, B.D., Savkin, D.E., Tolmachev, G.N., Air-temperature dependence of the ozone generation rate in the surface air layer, *Atmos. Ocean. Opt.*, 2018, vol. 31, no. 2, pp. 187–196.

Berezina, E.V., Moiseenko, K.B., Skorokhod, A.I., Elansky, N.F., and Belikov, I.B., Aromatic volatile organic compounds and their role in ground-level ozone formation in Russia, *Dokl. Earth Sci.*, 2017, vol. 474, no. 1, pp. 599–603.

Browne, E.C. and Cohen, R.C., Effects of biogenic nitrate chemistry on the NOx lifetime in remote continental regions, *Atmos. Chem. Phys.*, 2012, vol. 12, pp. 11917–11932. https://doi.org/10.5194/acp-12-11917-2012

Browne, E.C., Min, K.-E., Wooldridge, P.J., Apel, E., Blake, D.R., Brune, W.H., Cantrell, C.A., Cubison, M.J., Diskin, G.S., Jimenez, J.L., Weinheimer, A.J., Wennberg, P.O., Wisthaler, A., and Cohen, R.C., Observations of total $RONO_2$ over the boreal forest: NOx sinks and HNO_3 sources, *Atmos. Chem. Phys.*, 2013, vol. 13, pp. 4543–4562. https://doi.org/10.5194/acp-13-4543-2013

Derwent, R.G., Manning, A.J., Simmonds, P.G., Spain, T.G., and O'Doherty, S., Analysis and interpretation of 25 years of ozone observations at the Mace Head Atmospheric Research Station on the Atlantic Ocean coast of Ireland from 1987 to 2012, *Atmos. Environ.*, 2013, vol. 80, pp. 361–368. https://doi.org/10.1016/j.atmosenv.2013.08.003

Engvall-Stjernberg, A.-C., Skorokhod, A.I., Elansky, N.F., Paris, J.-D., Nédélec, P., and Stohl, A., Low concentrations of near-surface ozone in Siberia, *Tellus, Ser. B*, 2012, vol. 64, p. 11607. https://doi.org/10.3402/tellusb.v64i0.11607

Guenther, A., Hewitt, C.N., Erickson, D., Fall, R., Geron, C., Graedel, T., Harley, P., Klinger, L., Lerdau, M., Mckay, W.A., Pierce, T., Scholes, B., Steinbrecher, R., Tallamraju, R., Taylor, J., and Zimmerman, P., A global-model of natural volatile organic compound emissions, *J. Geophys. Res.*, 1995, vol. 100, no. D5, pp. 8873–8892. https://doi.org/10.1029/94JD02950

Hakola, H., Hellén, H., Tarvainen, V., Bäck, J., Patokoski, J., and Rinne, J., Annual variations of atmospheric VOC concentrations in a boreal forest, *Boreal Environ. Res.*, 2009, vol. 14, pp. 722–730.

Heimann, M., Schulze, E.D., Winderlich, J., Andreae, M., Chi, X., Gerbig, C., Kolle, O., Kübler, K., Lavric, J.V., Mikhailov, E., Panov, A., Park, S., Rödenbeck, C., and Skorochod, A., The Zotino Tall Tower Observatory (Zotto): Quantifying large scale biogeochemical changes in central Siberia, *Nova Acta Leopold. NF*, 2014, vol. 117, no. 399, pp. 51–64.

Hens, K., Novelli, A., Martinez, M., Auld, J., Axinte, R., Bohn, B., Fischer, H., Keronen, P., Kubistin, D., Nölscher, A.C., Oswald, R., Paasonen, P., Petäjä, T., Regelin, E., Sander, R., et al., Observation and modelling of HOx radicals in a boreal forest, *Atmos. Chem. Phys.*, 2014, vol. 14, pp. 8723–8747. https://doi.org/10.5194/acp-14-8723-2014

Kenagy, H.S., Sparks, T.L., Ebben, C.J., Wooldrige, P.J., Lopez-Hilfiker, F.D., Lee, B.H., Thornton, J.A., McDuffie, E.E., Fibiger, D.L., Brown, S.S., Montzka, D.D., Weinheimer, A.J., Schroder, J.C., Campuzano-Jost, P., Day, D.A., et al., NOx lifetime and NOy partitioning during winter, *J. Geophys. Res.*, 2018, vol. 123, pp. 9813–9827. https://doi.org/10.1029/2018JD028736

Kleinman, L., Lee, Y.-N., Springston, S.R., Lee, J.H., Nunnermacker, L., Weinstein-Lloyd, J., Zhou, X., and Newman, L., Peroxy radical concentration and ozone formation rate at a rural site in the southeastern United States, *J. Geophys. Res.*, 1995, vol. 100, no. D4, pp. 7263–7273. https://doi.org/10.1029/95JD00215

Kulmala, M., Suni, T., Lehtinen, K.E.J., Dal Maso, M., Boy, M., Reissell, A., Rannik, U., Aalto, P., Keronen, P., Hakola, H., Back, J.B., Hoffmann, T., Vesala, T., and Hari, P., A new feedback mechanism linking forests, aerosols, and climate, *Atmos. Chem. Phys.*, 2004, vol. 4, pp. 557–562. https://doi.org/10.5194/acp-4-557-2004

Lew, M.M., Rickly, P.S., Bottorff, B.P., Reidy, E., Sklaveniti, S., Leonardis, T., Locoge, N., Dusanter, S., Kundu, S., Wood, E., and Stevens, P.S., OH and HO_2 radical chemistry in a midlatitude forest: Measurements and model comparisons, *Atmos. Chem. Phys.*, 2020, vol. 20, pp. 9209–9230. https://doi.org/10.5194/acp-20-9209-2020

Liebmann, J., Sobanski, N., Schuladen, J., Karu, E., Hellen, H., Hakola, H., Zha, Q., Ehn, M., Riva, M., Heikkinen, L., Williams, J., Fischer, H., Lelieveld, J., and Crowley, J.N., Alkyl nitrates in the boreal forest: Formation via the NO_3^-, OH^- and O_3^- induced oxidation of biogenic volatile organic compounds and ambient lifetimes, *Atmos. Chem. Phys.*, 2019, vol. 19, pp. 10391–10403. https://doi.org/10.5194/acp-19-10391-2019

Liu, S.C., Trainer, M., Fehsenfeld, F.C., Parrish, D.D., Williams, E.J., Fahey, D.W., Hobler, G., and Murphy, P.C., Ozone production in the rural troposphere and the implications for regional and global ozone distributions, *J. Geophys. Res.*, 1987, vol. 92, no. D4, pp. 4191–4207. https://doi.org/10.1029/JD092iD04p04191

Moiseenko, K.B., Shtabkin, Yu.A., Berezina, E.V., and Skorokhod, A.I., Regional Photochemical surface-ozone sources in Europe and Western Siberia, *Izv., Atmos. Ocean. Phys.*, 2018, vol. 54, no. 6, pp. 545–557.

Moiseenko, K.B., Vasileva, A.V., Skorokhod, A.I., Belikov, I.B., Repin, A.Yu., and Shtabkin, Yu.A., Regional impact of ozone precursor emissions on NOx and O_3 levels at Zotto tall tower in central Siberia, *Earth Space Sci.*, 2021, vol. 8, p. e2021EA001762. https://doi.org/10.1029/2021EA001762

Moiseenko, K.B., Vasil'eva, A.V., Skorokhod, A.I., Shtabkin, Yu.A., Belikov, I.B., Repin, A.Yu., Photostationary equilibrium in the O_3–NO_x system and ozone generation according to ZOTTO tall tower data, *Atmos. Ocean. Opt.*, 2022, vol. 35, no. S1, pp. S125–S132.

Petersen, R., Holst, T., Molder, M., Kljun, N., and Rinne, J., Vertical distribution of sources and sinks of volatile organic compounds within a boreal forest canopy, *Atmos. Chem. Phys.*, 2023, vol. 23, pp. 7839–7858. https://doi.org/10.5194/acp-23-7839-2023

Pochanart, P., Akimoto, H., Kajii, Y., Potemkin, V.M., and Khodzher, T.V., Regional background ozone and carbon monoxide variations in remote Siberia/East Asia, *J. Geophys. Res.*, 2003, vol. 108, no. D1, p. 4028. https://doi.org/10.1029/2001JD001412

Schulze, E.-D., Vygodskaya, N.N., Tchebakova, N.M., Czimczik, C.I., Kozlov, D.N., Lloyd, J., Mollicone, D., Parfenova, E., Sidorov, K.N., Varlagin, A.V., and Wirth, C., The Eurosiberian Transect: An introduction to the experimental region, *Tellus, Ser. B*, 2002, vol. 54, no. 5, pp. 421–428. https://doi.org/10.3402/tellusb.v54i5.16678

Seinfeld, J.H. and Pandis, S.N., *Atmospheric Chemistry and Physics: From Air Pollution to Climate Change*, New York: John Wiley and Sons, 2016.

Sillman, S., Logan, J.A., and Wofsy, S.C., The sensitivity of ozone to nitrogen oxides and hydrocarbons in regional ozone episodes, *J. Geophys. Res.*, 1990, vol. 95, pp. 1837–1851. https://doi.org/10.1029/JD095iD02p01837

Skorokhod, A.I., Berezina, E.V., Moiseenko, K.B., Elansky, N.F., and Belikov, I.B., Benzene and toluene in the surface air of Northern Eurasia from TROICA-12 campaign along the Trans-Siberian railway, *Atmos. Chem. Phys.*, 2017, vol. 17, pp. 5501–5514. https://doi.org/10.5194/acp-17-5501-2017

Spirig, C., Guenther, A., Greenberg, J.P., Calanca, P., and Tarvainen, V., Tethered balloon measurements of biogenic volatile organic compounds at a boreal forest site, *Atmos. Chem. Phys.*, 2004, vol. 4, pp. 215–229. https://doi.org/10.5194/acp-4-215-2004

Taraborrelli, D., Cabrera-Perez, D., Bacer, S., Gromov, S., Lelieveld, J., Sander, R., and Pozzer, A., Influence of aromatics on tropospheric gas-phase composition, *Atmos. Chem. Phys.*, 2021, vol. 21, pp. 2615–2636.

Thorp, T., Arnold, S.R., Pope, R.J., Spracklen, D.V., Conibear, L., Knote, C., Arshinov, M., Belan, B., Asmi, E., Laurila, T., Skorokhod, A.I., Nieminen, T., and Petäjä, T., Late-spring and summertime tropospheric ozone and NO_2 in Western Siberia and the Russian Arctic: Regional model evaluation and sensitivities, *Atmos. Chem. Phys.*, 2021, vol. 21, pp. 4677–4697. https://doi.org/10.5194/acp-21-4677-2021

Trainer, M., Hsie, E.Y., McKeen, S.A., Tallamraju, R., Parrish, D.D., Fehsenfeld, F.C., and Liu, S.C., Impact of natural hydrocarbons on hydroxyl and peroxy radicals at a remote site, *J. Geophys. Res.*, 1987, vol. 92, no. D10, pp. 11879–11894. https://doi.org/10.1029/JD092iD10p11879

Trainer, M., Parrish, D.D., Buhr, M.P., Norton, R.B., Fehsenfeld, F.C., Anlauf, K.G., Bottenheim, J.W., Tang, Y.Z., Wiebe, H.A., Roberts, J.M., Tanner, R.L., Newman, L., Bowersox, V.C., Meagher, J.F., Olszyna, K.J., et al., Correlation of ozone with NOy in photochemically aged air, *J. Geophys. Res.*, 1993, vol. 98, pp. 2917–2925. https://doi.org/10.1029/92JD01910

Young, V.L., Kieser, B.N., Chen, S.P., and Niki, H., Seasonal trends and local influences on nonmethane hydrocarbon concentrations in the Canadian boreal forest, *J. Geophys. Res.*, 1997, vol. 102, no. D5, pp. 5913–5918. https://doi.org/10.1029/96JD03375

Translated by A. Nikol'skii